RAPID COMMUNICATIONS

PHYSICAL REVIEW B VOLUME 34, NUMBER 3 1 AUGUST 1986

Stacking structure and superconductivity in ruthenium-iridium bicrystal superlattices

Roy Clarke, F. Lamelas, and C. Uher
Department of Physics, University of Michigan, Ann Arbor, Michigan 48109

C. P. Flynn
University of Illinois at Urbana-Champaign, Urbana, Illinois 61801

J. E. Cunningham
AT&T Bell Laboratories, Holmdel, New Jersey 07733

(Received 1 May 1986)

The stacking structure and epitaxial ordering are studied in molecular-beam-epitaxy-grown Ru-Ir superlattices of wavelengths $\lambda = 10$, 41, and 62 Å. These samples span the fcc-hcp crossover previously found to occur when the Ir component is thinner than about 10 monolayers. Evidence for a new stacking sequence of period 3λ is found in the $\lambda = 41$ Å sample, possibly resulting from stacking faults in the Ir layers. The superconducting transition temperature is significantly higher in the 41-Å sample ($T_c = 0.19$ K) than in the 62-Å sample ($T_c = 0.15$ K), whereas the 10-Å sample is not superconducting down to 20 mK.

Artificial superlattices continue to provide interesting examples of solid-state systems in which the structure and composition are controlled on an atomic scale in order to obtain extraordinary physical properties. Previous studies have focused predominantly on superlattices derived from highly lattice-matched isostructural materials; for example, GaAs-$Al_xGa_{1-x}As$,[1] Nb-Ta,[2] and Gd-Y.[3]

Recently it has been demonstrated that under some circumstances high-quality superlattice growth is possible even when the crystal structures of the two components of the superlattice differ from each other.[4] In particular fcc-hcp "bicrystal" superlattices were fabricated at the University of Illinois by sequential molecular-beam-epitaxy deposition of Ir and Ru, respectively. Several aspects make this particular combination of metals favorable, most importantly the fcc(111)÷hcp(00.1) epitaxial relationship.[5] This factor, together with the fairly close (0.3%) matching of the nearest-neighbor distances in Ru and Ir, promotes the coherent growth of close-packed layers to form an essentially single-crystal three-dimensional heterostructure.

In this paper we investigate the structural ordering of Ru-Ir superlattices and the relationship to electronic properties such as resistivity and superconductivity. Particular reference is made to the intriguing observation[4] that when the Ir strata are very thin ($\lesssim$10 monolayers) the stacking within the Ir component takes an hcp configuration in contrast to the bulk fcc structure. Using x-ray diffuse scattering techniques we are able to identify very-long-range coherent stacking sequences in the vicinity of this crossover and to probe stacking faults associated with the fcc-hcp transition.

The Ru-Ir superlattices used for this study were electron-beam evaporated on $(11\bar{2}0)$ sapphire substrates held at 920 °C in an ultrahigh vacuum environment.[4] This particular orientation was preferred because the tetragonal symmetry of the $(11\bar{2}0)$ face inhibits the nucleation of domains with translation vectors rotated by $\pm 30°$.

Two samples, of wavelengths $\lambda = 41$ and 62 Å, were studied in detail. In both samples the Ru strata were intended to have a constant thickness of approximately 11 atomic planes (~24 Å), whereas an Ir stratum of about 8 atomic planes was aimed for in the former sample and about 15 atomic planes in the latter [see inset in Fig. 1(a)]. The total thickness of the superlattice films was approximately 2000 Å (~40 periods).

Diffuse scattering measurements were carried out on a Huber four-circle diffractometer with a 12-kW rotating-anode x-ray source. Graphite-monochromatized molybdenum radiation ($\lambda = 0.71$ Å) was found to be advantageous on account of its penetrating power. This facilitated transmission measurements without removing the film from the 0.5-mm-thick sapphire substrate. In this way *in situ* x-ray scans with diffraction vector parallel to the plane of the film could conveniently be made to probe the epitaxial ordering and long-period stacking arrangements.

The superconductivity measurements were made by monitoring the resistivity of the sample as it was cooled in a dilution refrigerator. A dc four-probe method was used. To prevent Joule heating, sample currents were kept in the 1-μA range and μ-metal shielding reduced magnetic fields at the sample to milligauss levels.

The inset in Fig. 1(b) shows an $(hk0)$ map of the x-ray scattering intensity from the $\lambda = 41$ Å Ru-Ir sample. The hexagonal symmetry of the close-packed metal layers is evident, as is the high degree of epitaxial ordering. The additional spots rotated $\pm 30°$ from {100} reflections are due to the nucleation problem mentioned above and are a factor of $\sim 10^3$ weaker than the principal {100} reflections. No further in-plane diffraction spots from the film are observed above the almost flat thermal diffuse background. The $\lambda = 62$ Å sample has an in-plane diffraction similar to that shown in the inset of Fig. 1(b).

The stacking arrangements of atomic planes in the superlattices were studied by making diffractometer scans through the {100} diffraction peak in the direction (c^*)

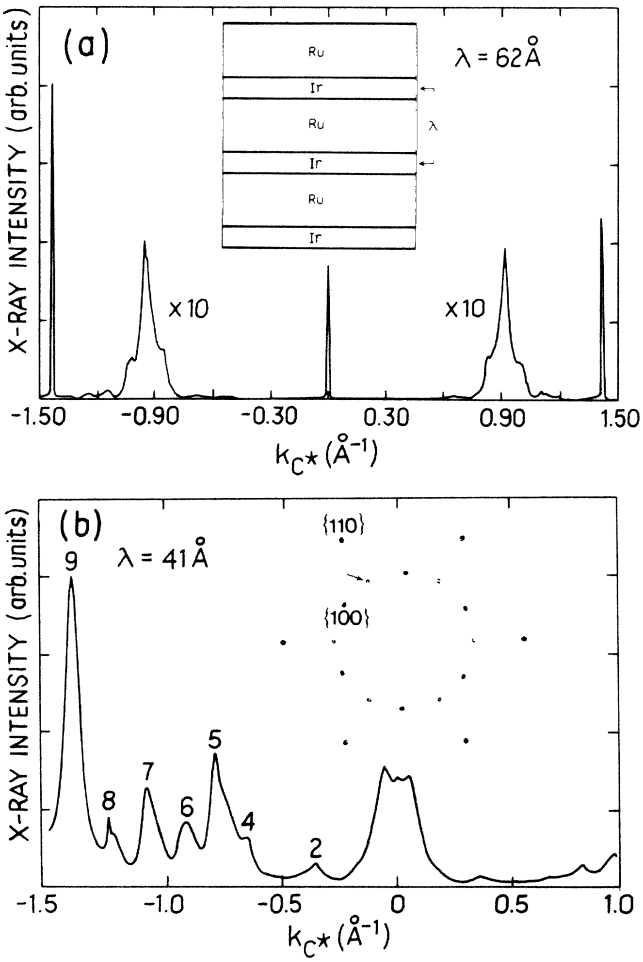

FIG. 1. (10l) scans for two Ru-Ir superlattices. k_c* is the projection of the diffraction vector on the c* axis (normal to the layers). The labels in (b) denote the l values of superlattice peaks. Inset in (a) shows a schematic layer structure of bicrystal superlattice samples. Inset in (b) is the in-plane diffraction pattern measured on $\lambda = 41$ Å sample. The peak arrowed originates from a nucleation of a small number of $\pm 30°$ domains.

normal to the layers, i.e., a (10l) scan. Figure 1(a) shows such a scan for the $\lambda = 62$ Å sample. The narrow prominent peaks at $k_c* = 2\pi(2\bar{d})^{-1} = 1.45$ Å^{-1} and $2\pi(3\bar{d})^{-1} = 0.96$ Å^{-1}, where $\bar{d}$ is the mean interplanar spacing, are associated with highly coherent hcp (*ABAB* . . .) and fcc (*ABCABC* . . .) stacking of Ru and Ir layers, respectively. In addition, sidebands are clearly seen split off from all principal peaks; the observed splitting of 0.10 Å^{-1} is consistent with their assignment to a superlattice modulation of 62 Å.

A similar (10l) scan for the $\lambda = 41$ Å sample [see Fig. 1(b)] reveals several interesting and unexpected differences in the stacking order compared to the longer-wavelength sample. Firstly, there is no obvious diffraction feature at $k_c* = 0.96$ Å^{-1} associated with fcc stacking in Ir. Secondly, the hcp peak at $k_c* = 1.45$ Å^{-1}, and indeed all the peaks in this scan, are substantially broader than the corresponding peaks in the $\lambda = 62$ Å sample [Fig. 1(a)].

The diffraction data for the $\lambda = 41$ Å sample [Fig. 1(b)] can best be interpreted in terms of a stacking arrangement in which the Ru and Ir components both exist predominantly in an hcp conformation. Thus, when the Ir strata are thin enough, on the order of 10 monolayers or less, there is a crossover to Ir hcp stacking from the bulk fcc structure. The peak broadening seen in Fig. 1(b) corresponds to a stacking correlation length of ~150 Å or about a factor of 5 less than for the 62-Å superlattice. We interpret this reduction in the correlation length of the 41-Å sample as being due to the presence of stacking faults in the Ir strata which may still retain a few fcc-type layers. Thus a typical Ir stratum in this sample may be stacked as follows: *ABAB//CBCB*, where the double slashes denote a stacking fault resulting from a remanent fcc package (*ABC*).

One additional interesting piece of information in Fig. 1(b) is related to a previously unobserved triplet of peaks around $k_c* = 0$. The triplet is composed of a principal {100} peak at $k_c* = 0$ flanked by two side peaks at ± 0.051 Å^{-1}. More detailed scans not shown here reveal weak high-order peaks at ± 0.102 Å^{-1}, etc. This set of Fourier components corresponds precisely to a 3λ periodicity superposed on the normal superlattice modulation of wavelength λ. The exact origin of this unexpectedly large commensurate (locked-in) superstructure is unclear at present but we tentatively suggest one mechanism by which such an ordering could arise. If a small amount of fcc stacking still persists in the $\lambda = 41$ Å sample then one stacking fault (or fcc package) per Ir layer would have the effect of shifting the phase of the stacking sequence by $2\pi/3$. Thus the full sequence would repeat after 3 cycles, i.e., in a distance of 3λ. We envisage a complete stacking sequence such as *ABAB//CBCB* . . . *CBCB//ACAC* . . . *ACAC//ABAB* . . . , where the dots represent the hcp Ru packages. Regarding the data of Fig. 1(b), it should be noted that the stacking correlation length given by the inverse width of the (10l) peaks is on the same order as the true 3λ repeat distance (123 Å). Thus, there is some randomness as to the placement of the stacking fault within each Ir layer.

A theoretical argument for the appearance of such long-period stacking-fault configurations has recently been proposed by Redfield and Zangwill.[6] In their analysis, Friedel-like oscillatory interactions associated with the interfaces of the metallic superlattice stabilize polytypes which are intermediate between hcp and fcc. When the compositional layer thickness is less than the Friedel wavelength, a stacking fault can occur on every atomic plane. As pointed out in their study this could account for the conversion of thin Ir strata from fcc to hcp.

A further type of x-ray scan was carried out on each sample in order to characterize the quality of the layering and the presence of interfacial alloying. Figure 2(a) shows (00l) scans for the $\lambda = 41$ and 62 Å samples; the diffraction vector is strictly perpendicular to the layers.

Immediately, one can judge from the many Fourier components that the interfaces between Ru and Ir strata are very sharp. We have performed detailed structure-factor modeling for both samples and find that the envelope of the (00l) profile is quite sensitive to the range of intermixing at the interface. On the other hand, the inten-

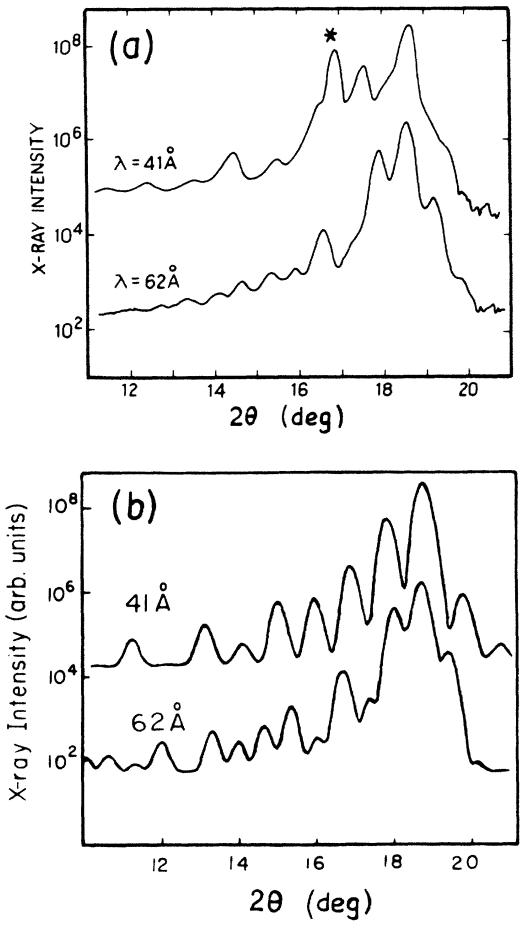

FIG. 2. (00l) diffraction profiles for two Ru-Ir superlattice samples: (a) measured; (b) calculated according to the model discussed in the text including instrumental broadening. The peak marked (*) is a sapphire ($11\bar{2}0$) substrate peak. The upper trace is displaced vertically by two orders of magnitude for clarity.

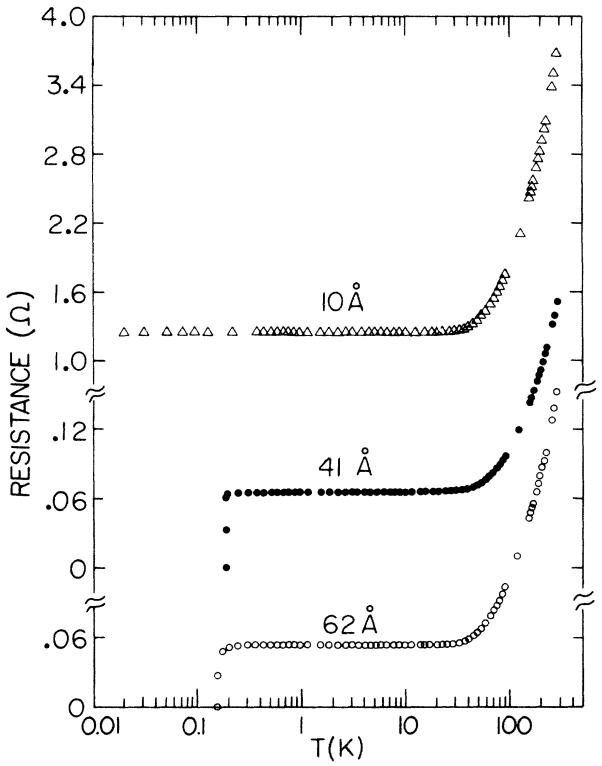

FIG. 3. Resistance vs temperature for three Ru-Ir superlattice samples. The data are offset vertically for clarity. The large resistance of the 10-Å sample is due to a geometrical factor; the actual sheet resistance is given in Table I.

sity ratios of individual superlattice peaks are very sensitive to the average number of layers of each constituent within the unit cell. We find the best fit to the observed profile with sequences containing on average 12 atomic planes of Ru and 16 of Ir for the 62-Å sample, and 11 atomic planes of Ru and 9 of Ir for the 41-Å sample. These figures are to within ± 1 monolayer of the intended composition ratios. The best-fit envelope profile is obtained with intermixing confined to a single interplanar spacing with only a small concentration (~15%) of Ru in Ir, and vice versa, in the two interfacial monolayers. The intensities calculated from our model are shown in Fig. 2(b). Although the fits are very promising, some improvement would be obtained by including disorder in the form of a slightly variable number of layers per stratum.

Finally, we report on the first measurements of the superconducting behavior of Ru-Ir superlattices. Figure 3 shows the temperature dependence of the resistance, measured parallel to the layers, of the 41- and 62-Å samples together with data for a very short wavelength sample $\lambda = 10$ Å. All three have a typical metallic character and do not show any of the localization effects observed in other, less coherent, bicrystal heterostructures such as Mo-Ni.[7] All samples have residual resistivity ratios (RRR) significantly greater than unity (see Table I).

Since both Ru and Ir are known to be superconducting, albeit at fairly low temperatures (0.49 and 0.14 K, respectively), the superlattices represent a proximity-coupled structure and it is not surprising that both the 41- and 62-Å samples undergo transitions to the superconducting state. Interestingly, we find that the 41-Å sample has a T_c about 22% higher than that of the 62-Å sample and this is likely due to its thinner iridium layers. The possibility exists, however, that the higher T_c of the 41-Å sample might also be associated with the metastable hexagonal structure of Ir.

The very-short-modulation-wavelength sample $\lambda = 10$ Å surprisingly did not show superconducting behavior down to ~20 mK. The x-ray data here reveal only one weak satellite indicative of a sinusoidal composition modulation; this is not unexpected considering that each monolayer

TABLE I. Some characteristic parameters of Ru-Ir bicrystal superlattices.

Wavelength	Structure	*RRR*	R (Ω/□)	T_c (K)
10 Å	Alloy	3.16	0.508	≤18 mK
41 Å	hcp Ru–hcp Ir	3.53	0.403	0.1919
62 Å	hcp Ru–fcc Ir	4.02	0.364	0.1570

neighbors an interface in this sample. Random Ru-Ir alloys of comparable composition are known to superconduct[8] at about 0.2 K, a temperature which is an order of magnitude higher than to where the $\lambda = 10$ Å sample was cooled without any trace of superconductivity. We speculate that the interfacial overlap in this sample drastically suppresses the density of states and precludes the onset of superconductivity. A wider range of these structures should be investigated to ascertain the role of metastability and disorder on the superconducting behavior.

In summary, Ru-Ir bicrystal superlattices ($40\ \text{Å} \lesssim \lambda \lesssim 60$ Å) show a remarkable degree of structural coherence with minimal interfacial alloying. The crossover from fcc Ir structure to hcp in short wavelength samples ($\lambda \approx 40$ Å) is found to be accompanied by a lock in of the stacking periodicity to 3λ. This behavior is reminiscent of polytypism observed in some other layered materials[9] and discussed in a recent theoretical paper by Bruinsma and Zangwill.[10] It is possible that this crossover might be responsible also for an enhancement of T_c observed on the 41-Å modulation wavelength Ir-Ru sample. It would be of interest to carry out further studies on samples near the fcc-hcp crossover.

We acknowledge the support of the U.S. Army Research Office, Grant No. DAAG-29-83-K-0131, of the NSF, Low Temperature Physics Grant No. DMR 850392 (C.U.), and of the University of Illinois Materials Research Laboratory under NSF Grant No. DMR 83-16981.

---

[1]D. Dingle, H. L. Störmer, A. C. Gossard, and W. Wiegman, Appl. Phys. Lett. **33**, 665 (1978).

[2]S. M. Durbin, J. E. Cunningham, M. E. Mochel, and C. P. Flynn, J. Phys. F **11**, L223 (1981).

[3]J. Kwo, E. M. Gyorgy, D. B. McWhan, M. Hong, F. J. DiSalvo, C. Vettier, and J. E. Bower, Phys. Rev. Lett. **55**, 1402 (1985).

[4]J. E. Cunningham and C. P. Flynn, J. Phys. F **15**, L221 (1985).

[5]J. Q. Zheng, J. B. Ketterson, and G. P. Felcher, J. Appl. Phys. **53**, 3624 (1982).

[6]A. C. Redfield and A. M. Zangwill (unpublished).

[7]C. Uher, R. Clarke, G.-G. Zheng, and I. K. Schuller, Phys. Rev. B **30**, 453 (1984).

[8]G. Riblet and M. A. Jensen, Physica **55**, 622 (1971).

[9]A. R. Verma and P. Krishna, *Polymorphism and Polytypism in Crystals* (Wiley, New York, 1966).

[10]R. Bruinsma and A. Zangwill, Phys. Rev. Lett. **55**, 214 (1985).